Original Study

Clinical Applicability of a Preoperative Angular Insertion Depth Prediction Method for Cochlear Implantation

*Christoph Rathgeb, †‡Marco Dematté, †§Abraam Yacoub, †Lukas Anschuetz, ||Franca Wagner, †Georgios Mantokoudis, *†Marco Caversaccio, and *†Wilhelm Wimmer

**Hearing Research Laboratory, Artificial Organs Center for Biomedical Engineering Research; †Department of Otorhinolaryngology, Head and Neck Surgery, Inselspital, Bern University Hospital, University of Bern; ‡Department of Otorhinolaryngology, Head & Neck Surgery, Head and Neck and Sensory Organs Department, Sant'Orsola-Malpighi Hospital, University of Bologna, Bologna, Italy; §Department of Otorhinolaryngology, Faculty of Medicine, Ain Shams University, Cairo, Egypt; and ||Department of Diagnostic and Interventional Neuroradiology, Inselspital, University Hospital and University of Bern, Bern, Switzerland*

Objective: Evaluation of the accuracy and clinical applicability of a single measure cochlear implant angular insertion depth prediction method.

Background: Cochlear implantation outcomes still vary extensively between patients. One of the possible reasons could be variability in intracochlear electrode array placement. For this reason, single measure methods were suggested to preoperatively predict angular insertion depths. Based on a previously performed accuracy study in human temporal bones, we were interested in determining the extent to which the method could be applied in a clinical setting.

Methods: A retrospective analysis was performed on pre- and postoperative radiographic images of 50 cochlear implant recipients. Preoperatively predicted angular insertion depths were compared with angular insertion depths measured on postoperative ground truth. The theoretical prediction error was computed under the assumption that all achieved insertions were matching the preoperatively assumed linear insertion depth. More importantly, the clinical prediction error was assessed using two different software tools performed by three experienced surgeons.

Results: Using the proposed method we found a theoretical prediction error of 5 degrees (SD = 41 degrees). The clinical prediction error including the cases with extracochlear electrodes was 70 degrees (SD = 96 degrees).

Conclusions: The presented angular insertion depth prediction method is a first practical approach to support the preoperative selection of cochlear implant electrode arrays. However, the presented procedure is limited in that it is unable to predict the occurrence of insertion results with extracochlear electrodes and requires user training.

Key Words: A value—Basal turn diameter—Cochlear base length—Cochlear duct length—Escude's equation—Otoplan.

Otol Neurotol **40:**xxx–xxx, 2019.

While cochlear implants (CIs) can significantly improve speech understanding, many CI receivers do not achieve optimal speech recognition even after many years (1). One of the reasons influencing the outcome variability may be the placement of the CI electrode array inside the cochlea. Misplaced electrode arrays can cause frequency mismatch and lead to reduced speech understanding (2). Over inserted electrode arrays can cause trauma to sensitive intracochlear structures (3), while under inserted electrode arrays have a reduced number of functional stimulation channels (4,5). In addition to the surgical challenges for electrode array insertion, the high variability in the cochlear morphology impedes an electrode array placement at a specific insertion depth (6–8).

The insertion depth can be expressed with two parameters: the linear insertion depth (LID) and the angular insertion depth (AID). The LID indicates the length of the electrode array partition (in mm) inserted into the cochlea. The AID describes the angular position (in degrees) of the most apical electrode inside the cochlea. A preoperative AID prediction can be used clinically to achieve desirable insertion depths for patients with residual hearing or malformations, to avoid tonotopic mismatch, bilateral mismatch between two implants in one patient and over- or under-insertion of the electrode array. Preoperative image-based approaches for the prediction of the cochlear duct length were proposed (9,10).

Address correspondence and reprint requests to Wilhelm Wimmer, Ph.D., ARTORG Center for Biomedical Engineering Research, University of Bern, Bern, Switzerland;
E-mail: wilhelm.wimmer@artorg.unibe.ch

This research project was supported by the Eurostars E! 11597 RCI research grant.

The authors have no conflicts of interest to disclose.

Supplemental digital content is available in the text.

DOI: 10.1097/MAO.0000000000002304

Escudé et al. (9) proposed a logarithmic equation that correlates the cochlear base length (CBL), also known as the ''A'' value (8), with the lateral wall of the cochlea. However, the used equation is based on a two-dimensional spiral form and therefore does not entirely reflect the three-dimensional morphology of the cochlea. Alexiades et al. (10) adapted Escudé's equation to predict the full and two-turn cochlear duct length, taking into account that the center of the electrode array is displaced relative to the cochlear lateral wall. Anschuetz et al. (11) refitted Escudé's equation with three-dimensional measurements of lateral wall electrode arrays, enabling the estimation of arbitrary AID values.

With this simple method, in a clinical environment, the prediction error can be influenced by several sources: 1) landmark inaccuracies caused by slicing angle, 2) image artifacts, 3) intraobserver variability (12), 4) inaccuracies caused by the equation, and 5) discrepancies in surgical outcomes. In addition, there are factors that cannot be controlled, such as new temporal bone formation or fractures, otosclerosis, and other forms of cochlear anomalies that can influence the electrode array insertion depth. Even patients with no radiographic indication of malformations can receive an incomplete electrode array insertion (13). In a previous temporal bone study, the accuracy of a single-measure AID prediction method was evaluated under controlled conditions (i.e., defined insertion trajectory and insertion stop) (11). The primary objective of this study was to evaluate the accuracy and applicability of the prediction method based on clinical data. The secondary objective was to compare the prediction accuracy of three clinicians who performed measurements with two different commercially available software tools.

MATERIALS AND METHODS

Study Design and Data Collection

We performed a retrospective analysis on pre- and postoperative computed tomography (CT) and cone beam computed tomography (CBCT) scans of 50 CI patients. The local institutional review board (Reference No. 2017–01462) approved data collection and analysis. All patients were implanted with the same CI model with lateral wall electrode arrays (Synchrony + Flex^{28}, Med-El, Innsbruck, Austria) between 2015 and 2017. Only data from patients with normal cochlear anatomy and no obstructions of the cochlea were included for analysis. The data set contained images of 20 left and 30 right ears of 26 female and 24 male subjects aged between 21 and 88 years (average age, 55 yrs; standard deviation [SD], 17 yrs). The radiographic scans (in total 100) had a voxel size of at least 0.4 mm^3 (refer to supplementary digital content 1, http://links.lww.com/MAO/A793, for more details about the imaging protocols).

Cochlear Landmarks

The measurements performed in this study included the identification of the following anatomical landmarks on radiographic images: 1) the center of the round window, 2) the center of the modiolus in the basal turn, 3) the helicotrema, and 4) the opposite outer cochlear wall (Fig. 1B). To identify these landmarks, the cochlear basal turn and cross-section through the modiolus need to be visualized using oblique slices in a multiplanar (MPR) viewer (Fig. 1B) (14).

Ground Truth Measurements

A reference data set was created to provide a ground-truth for error evaluation. To minimize errors caused by repeated landmark selection as well as impeded landmark identification in the postoperative image (i.e., presence of electrode array and image artifacts), the postoperative images of each patient were registered with the preoperative images using a normalized mutual information algorithm (Fig. 1A) (15) (Amira, Thermo Scientific, USA). Based on the cochlear landmarks, identified in the preoperative images, a cochlear coordinate system was computed (14,16). The image registration process allowed the preoperative cochlear landmarks to be reused in the postoperative images. In the preoperative images, the CBL was calculated along the x-axis of the cochlear coordinate system (Fig. 1B).

Angular Insertion Depth Prediction

In the postoperative images, the actual AID was calculated from the coordinates of the most apical electrode array (Fig. 1C). We used the equation presented in Anschuetz et al. (11), to predict the AID for a given LID and CBL:

$$\mathrm{AID} = 248 \cdot \left(e^{\mathrm{LID}/(2.43 \cdot \mathrm{CBL})} - 1\right) \quad (1)$$

The equation predicts the angular position of the center of the most apical electrode, not the silicon tip of the electrode array, which is undetectable in postoperative scans. Therefore, the electrode array length needs to be adapted for the prediction. With the array type investigated in this study (Flex^{28}, i.e., total array length of 28 mm) an effective length of 26.95 mm (a reduction of 1.05 mm, from the silicon tip to the center of the most apical electrode) was used (see Fig. 2A).

Evaluation of Insertion Outcome

In the postoperative image data, the insertion outcomes were grouped in two categories: 1) full insertion, i.e., all electrodes within the cochlea and 2) partial insertion, i.e., not all electrodes within the cochlea as indicated in the CT images (Fig. 2B).

Evaluation of Theoretical Prediction Error

The assumption that the electrode array length corresponds to the LID only applies if the stopper is exactly at the level of the round window (Fig. 2B). When the electrode array is not fully inserted, the LID differs from the length of the electrode array, which affects the AID prediction error. To take this effect into account, the theoretical AID prediction error is calculated based on the actual LID measured in the postoperative images (Fig. 2C). The actual LID was automatically computed using the position of the most intracochlear basal electrode and the round window landmark.

Evaluation of Clinical Prediction Error

For the evaluation of the clinical prediction error, three experienced otologists independently measured the CBL in the preoperative images with two different software tools each: 1) a clinical standard MPR viewer software (Sectra PACS, Sweden [Fig. 3A]), and 2) a planning software developed together with the University of Bern and Inselspital in Bern (OtoPlan, CAScination AG, Bern, Switzerland [Fig. 3B]). Before the measurements, the surgeons were trained in the use of the software tools and the identification of cochlear landmarks.

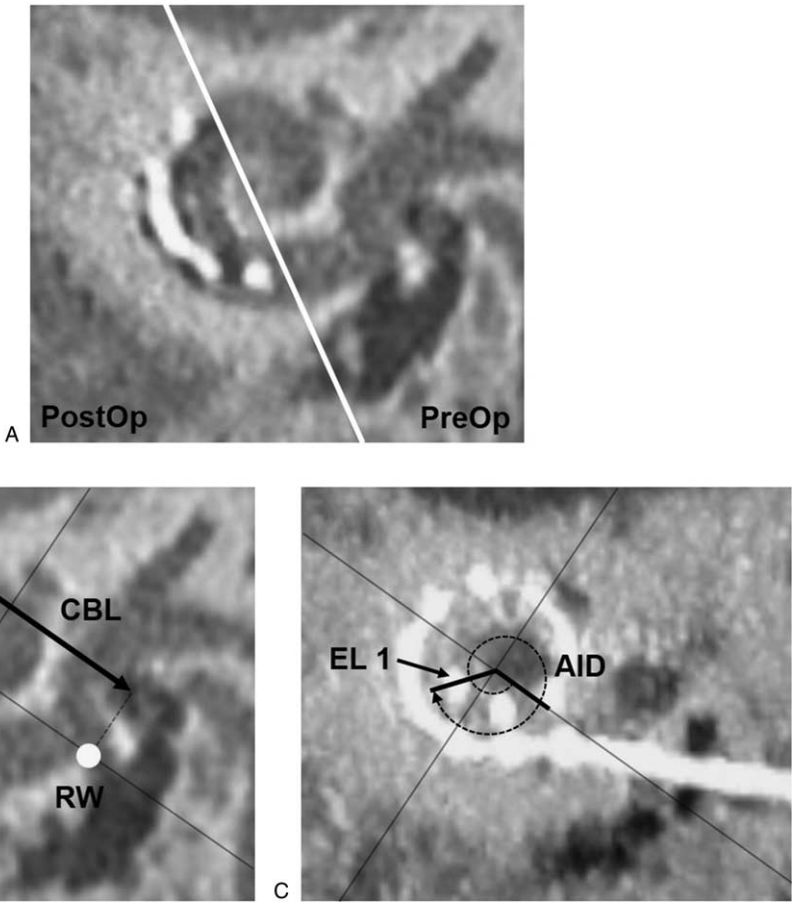

FIG. 1. *A*, Example of registered preoperative and postoperative CT scans (subject 1). *B*, Landmark identification of the round window center (RW), the center of the modiolus in the basal turn (C), and the lateral wall intersection (LW). The cochlear base length (CBL) is defined as the distance between the RW and LW landmarks. *C*, Visualization of the postoperative angular insertion depth (AID) based on the most apical electrode (EL1) using a maximum intensity projection.

In total, this resulted in 300 measurements of CBL values that were used to predict the AID. To assess accuracy, the predicted AID values were compared with the reference ground truth AID values. The AID differences were estimated using a linear mixed-effects model, with a fixed effect of the measurement method (i.e., standard viewer versus planning software) and random effects for subject to account for repeated measures as well as method nested within observer to account for autocorrelations. The interobserver variability was described using a two-way mixed effects intra class correlation (ICC), measured with the R environment (psych package). Additionally the time was recorded for each measurement.

Calculation Example

A subject has a CBL of 9.5 mm. Under the assumption that the electrode array (Flex[28]) can be completely inserted (i.e., up to the silicon stopper), a LID of 26.95 mm is used for the estimation:

$$\mathrm{AID_c} = 248 \cdot \left(e^{26.95/(2.43\ \cdot\ 9.5)} - 1\right) = 549^\circ \quad (2)$$

In the postoperative images of the subject an AID of 485 degrees is measured. The estimation was off by 64 degrees (clinical prediction error). However, the postoperative images of this subject indicate that 1 mm of the array remained outside the cochlea. To evaluate how the equation would have estimated the AID in this case, the calculation is repeated for the reduced linear insertion depth (26.95 – 1.00 = 25.95 mm):

$$\mathrm{AID_T} = 248 \cdot \left(e^{25.95/(2.43\ \cdot\ 9.5)} - 1\right) = 515^\circ \quad (3)$$

This estimation yields a better result (30 degrees error), but cannot be considered as clinically relevant, because it refers to the postoperative imaging results (theoretical prediction error). However, it validates how well the equation is capturing the relationship between LID, CBL, and AID.

RESULTS

Insertion Outcome

The image quality was sufficient in all cases to identify the cochlear landmarks and electrodes. Postoperative analysis classified 78% (n = 39) as full insertions. In 22% of the cases (n = 11) radiological assessment

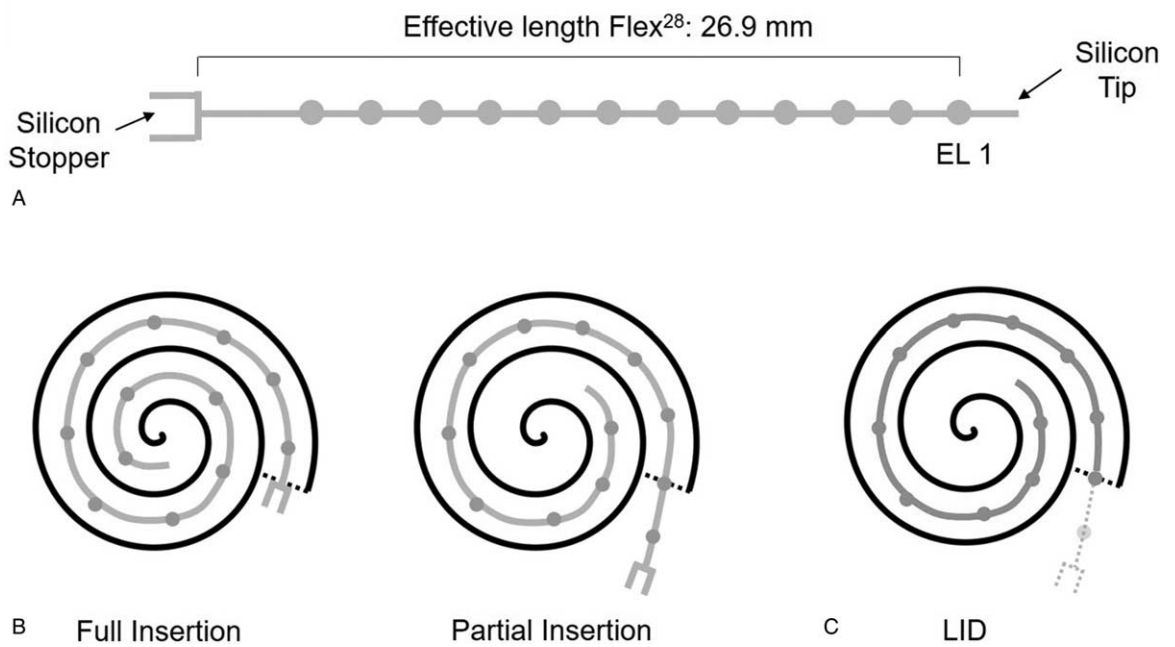

FIG. 2. *A*, Schematic visualization of a Flex[28] electrode array, showing the effective length between the stopper and EL1 is most apical electrode. *B*, Insertion outcome categories: full insertion and partial insertion. *C*, Linear insertion depth (LID) of a partially inserted electrode array.

showed extracochlear electrode contacts. There were nine cases with one or two extracochlear contacts, one case with three extracochlear contacts, and one case with six extracochlear contacts (refer to supplementary digital content 2, http://links.lww.com/MAO/A794, for more details). The average AID value measured on the post-operative images was 512 degrees (SD = 92 degrees). The CBL measured on the ground truth data set had an average of 9.0 mm (SD = 0.5 mm, min = 7.5 mm, max = 10.1 mm). In the cases with extracochlear electrode arrays, the CBL was 8.9 mm (SD = 0.5 mm, min = 7.5 mm, max = 9.49 mm) and in cases of full insertions 9.1 mm (SD = 0.5 mm, min = 8.1 mm, max = 10.1 mm).

Theoretical Prediction Error

The theoretical AID prediction error was 5 degrees (SD = 41 degrees) indicating that the differences were small and not statistically significant ($p = 0.37$) (Fig. 4). The difference between the electrode array length and the actual LID was −1.62 mm (SD = 0.94 mm) for the full insertions and −6.37 mm (SD = 3.18 mm) for the cases with extracochlear electrodes.

Clinical Prediction Error

The analysis showed that the surgeons overestimated the AID with the clinical standard viewer software by 67 degrees (SD = 95 degrees) and the custom planning software by 73 degrees (SD = 96 degrees). The predicted

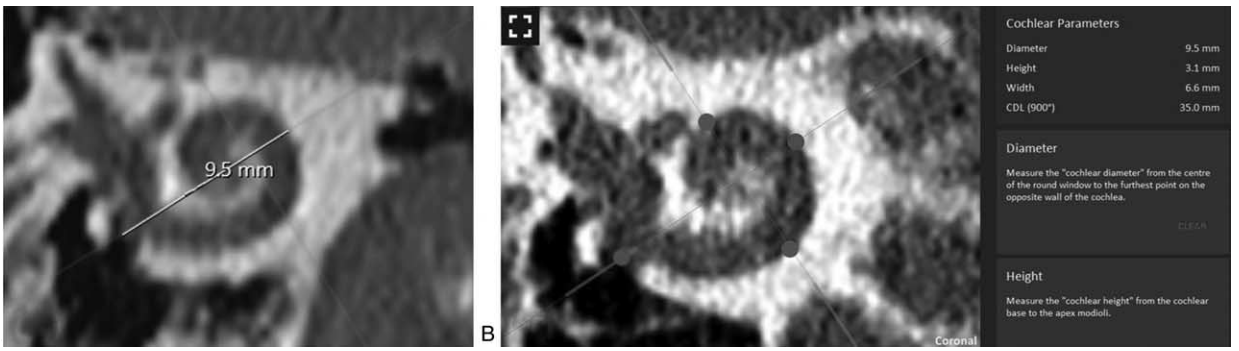

FIG. 3. *A*, Cochlear base length (CBL) assessed with conventional standard viewer. After visualizing the basal turn, the CBL is manually measured with an integrated ruler tool. *B*, The custom planning software guides the user through each step for landmark identification. Based on the landmark coordinates the CBL is calculated automatically.

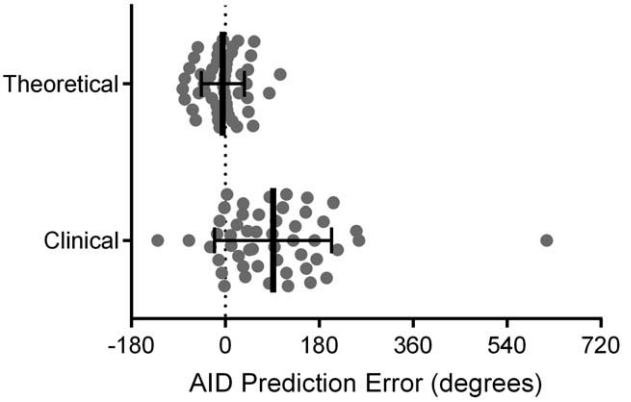

FIG. 4. Comparison between the theoretical and clinical angular insertion depth (AID) prediction errors. The theoretical prediction error is computed based on the actual linear insertion depth (LID) measured in the postoperative images, while the clinical prediction error is computed under the assumption that the LID is always equivalent to the electrode array length. A positive error indicates that the actual angular insertion depth was smaller than predicted. The bars show mean errors and standard deviations.

values using the two methods were significantly different from the ground truth values ($p < 0.001$). The two measurement methods showed no statistically significant difference ($p = 0.44$). The interobserver variability using the clinical standard viewer software and the custom planning software showed an ICC coefficient of 0.79 and 0.87, respectively. The surgeons reported an average time of 10 minutes per measurement, where both measurement tools required the same amount of time.

DISCUSSION

The presented study evaluated the clinical applicability of a single-measure preoperative AID prediction method (11) with the following two main findings: 1) the theoretical AID prediction error, i.e., the error that can be achieved under optimal conditions, is 5 degrees (SD = 41 degrees) and 2) in a clinical setting, the prediction error increases to 70 degrees (SD = 96 degrees) due to the occurrence of extracochlear electrode arrays. It is important to keep in mind that the described prediction method uses a simplified model. The precision of the prediction in this study was almost three times higher with the corrected LID (theoretical error, SD = 41 degrees) and 6.5 times higher under clinical conditions (SD = 96 degrees) than the precision (SD = 15 degrees) of the preclinical evaluation (11), which we consider to be performed under optimal conditions.

The main factors that can influence the clinical AID prediction error are 1) the occurrence of partial insertions and 2) the observer variability in CBL assessment. Comparison of the theoretical AID with the clinical AID prediction error illustrates the influence of extracochlear electrode arrays on the prediction accuracy. The insertion outcome evaluation showed that 78% were classified as full and 22% were classified as partial insertions which is slightly higher than the rate of 13% reported in a previous study (17), but matches the estimation of Timm et al. (18), who evaluated data of 272 CI patients and indicated the Flex^{28} electrode array to be of applicable size in 76.8% of the cases. The question arises regarding why these partial insertions occur even though there are no visible obstructions in the cochlea. Possible reasons could be 1) the increasing resistance from a certain insertion depth, 2) unfavorable insertion angles (e.g., non-tangential alignment with the centerline of the scala tympani), or 3) cochleae that were too small for the Flex^{28} electrode array, which was not the case in our data set. In addition, other factors not associated with cochlear morphology have to be considered when interpreting our data. 4) We applied a quite rigorous radiological approach for the assessment of extracochlear electrodes. The situation perceived by the surgeon during insertion might be different from the radiological assessment. For example, the visibility of the round window niche/bony overhang and the viewing angle during surgery could introduce discrepancies. While the surgeon confirms a full insertion, one electrode contact could appear as extracochlear in the postoperative radiologic view. This could have been the case in six of the 11 cases, presenting one extracochlear electrode array. 5) In our clinic, a conservative insertion approach is followed, where, if desired, surgeons stop at the first point of resistance to avoid exceeding insertion forces. This option is considered in the case with one or two electrode contacts remaining outside the cochlea. 6) Ultimately, electrode migration could have occurred in one of the 50 subjects. The data set contained one outlier (subject 9) with a clinical prediction error of 613 degrees. This subject had the smallest cochlea (CBL = 7.5 mm) in the data set, resulting in a high AID prediction of 834 degrees. However, a much smaller AID of 218 degrees was measured on the postoperative scans. The surgical report showed that two electrodes were classified as extracochlear. However, the postoperative analysis indicated a total of six extracochlear electrodes, possibly explained by electrode array migration. In this patient, a revision surgery is indicated. Extracochlear electrodes in the vicinity of the round window are not necessarily nonfunctional. A comparison with audiological fitting data showed that among the 11 cases with radiologically assessed extracochlear electrodes, two patients had functional stimulation channels at the extracochlear electrode contact closest to the round window (subjects 3 and 5).

The average CBL of 9.0 mm (SD = 0.5 mm) and AID of 512 degrees (SD = 92 degrees) are comparable to those of other studies (19,20), which indicates that our data set represents a normal distribution of patients. In the literature, similar logarithmic equations for the prediction of the LID as a function of the expected AID and CBL (9–11) were presented. However, the difference between these equations has only a small impact on the overall accuracy, if the datasets contain partial insertions.

Other studies showed (12) that there is a significant interobserver variability in CBL assessment when

measured on standard and MPR views. Both software tools used in this study provide MPR reconstruction and statistical analysis showed that there is no significant difference in the AID prediction error between the standard viewer and the custom planning software ($p = 0.44$). Interobserver variability was low for both the standard viewer (ICC = 0.79) and the custom planning software (ICC = 0.87), indicating that surgeons were well trained and familiar with the MPR viewer handling. While the standard viewer can be used for any sort of image consultation, the custom planning software is specifically designed to guide the user through the cochlear landmark identification process, which improves the usability reflected in the higher ICC score. Timewise, the methods were comparable with an average of 10 minutes per measurement, which involved the visualization of the cochlea and the identification of the cochlear landmarks.

The image data sets were acquired with different modalities (CT, CBCT), different protocols (different resolutions), and in different centers (Inselspital Bern or external). The image quality was sufficient on all samples to identify the required landmarks and to localize the electrodes. However, the difference in resolution from a CT scan with a resolution of $0.156 \times 0.156 \times 0.2$ to a CBCT scan with resolution of $0.4 \times 0.4 \times 0.4$ is not negligible. While the high variation of resolution might have an effect on the accuracy assessment, this is what can be expected in a clinical setting.

A possible application is given for Mondini dysplasia (maximum AID of 1.5 turns or 540 degrees) or common cavity malformations (maximum AID of 1 turn or 360 degrees). In such cases, a preoperative estimation proved valuable in our department to avoid the unnecessary opening of sterile packed implants, while maximizing cochlear coverage. However, further investigations are needed to show the validity of the equation in the mentioned cases. The prediction method relies on accurate CBL and cochlear landmark identification, which is only achievable through training. Automated CBL and cochlear landmark identification (21) can therefore potentially reduce time and training effort. In this study, only electrode arrays of one type from a single manufacturer were used. Further tests are required to evaluate the applicability of the presented AID prediction method to other lateral wall electrode arrays.

Our study is limited in that the data were analyzed retrospectively. Therefore, we cannot necessarily apply the estimation method in a prospective way, e.g., with instructions to fully insert arrays even if resistance is met. A major limitation of the presented estimation approach remains the uncertainty to account for partial insertions. The AID prediction error is strongly dependent on the insertion result. Therefore, methods capable of predicting partial insertion could significantly improve overall accuracy. In addition, the preoperative selection of cochlear implant electrode arrays could be further improved by methods that allow preoperative planning of ideal insertion trajectories and intraoperative constriction of insertion forces to such ideal insertion trajectories (22).

CONCLUSION

The presented prediction method could be a practical approach to support the preoperative selection of electrode arrays for cochlear implants. However, the presented procedure is limited in that it is unable to predict the occurrence of insertion results with extracochlear electrode arrays.

REFERENCES

1. Pisoni D, Kronenberger W, Harris M, Moberly A. Three challenges for future research on cochlear implants. *World J Otorhinolaryngol Head Neck Surg* 2017;3:240–54.
2. Buchman C, Dillon M, King R, Adunka M, Adunka O, Pillsbury H. Influence of cochlear implant insertion depth on performance: a prospective randomized trial. *Otol Neurotol* 2014;35:1773–9.
3. Eshraghi A, Nazarian R, Telischi F, Rajguru S, Truy E, Gupta C. The cochlear implant: historical aspects and future prospects. *Anat Rec (Hoboken)* 2012;295:1967–80.
4. Rader T, Döge J, Adel Y, Weissgerber T, Baumann U. Place dependent stimulation rates improve pitch perception in cochlear implantees with single-sided deafness. *Hear Res* 2016;339:94–103.
5. Schatzer R, Vermeire K, Visser D, Krenmayr A, Kals M, Voormolen M. Electric-acoustic pitch comparisons in single-sided-deaf cochlear implant users: frequency-place functions and rate pitch. *Hear Res* 2014;309:26–35.
6. Avci E, Nauwelaers T, Lenarz T, Hamacher V, Kral A. Variations in microanatomy of the human cochlea. *J Comp Neurol* 2014;522:3245–61.
7. Kawano A, Seldon HL, Clark GM. Computer-aided three-dimensional reconstruction in human cochlear maps: measurement of the lengths of organ of Corti, outer wall, inner wall, and Rosenthal's canal. *Ann Otol Rhinol Laryngol* 1996;105:701–9.
8. Hardy M. The length of the organ of corti in man. *Am J Anatomy* 1938;62:291–311.
9. Escudé B, James C, Deguine O, Cochard N, Eter E, Fraysse B. The size of the cochlea and predictions of insertion depth angles for cochlear implant electrodes. *Audiol Neurootol* 2006;11 (suppl):27–33.
10. Alexiades G, Dhanasingh A, Jolly C. Method to estimate the complete and two-turn cochlear duct length. *Otol Neurotol* 2015;36:904–7.
11. Anschuetz L, Weder S, Mantokoudis G, et al. Cochlear implant insertion depth prediction: a temporal bone accuracy study. *Otol Neurotol* 2018;39:e996–1001.
12. Iyaniwura J, Elfarnawany M, Riyahi-Alam S, Sharma M, Kassam Z, Bureau Y. Intra- and interobserver variability of cochlear length measurements in clinical CT. *Otol Neurotol* 2017;38:828–32.
13. Lee J, Nadol J, Eddington D. Factors associated with incomplete insertion of electrodes in cochlear implant surgery: a histopathologic study. *Audiol Neurootol* 2011;16:69–81.
14. Verbist B, Skinner M, Cohen L, et al. Consensus panel on a cochlear coordinate system applicable in histologic, physiologic, and radiologic studies of the human cochlea. *Otol Neurotol* 2010;31:722–30.
15. Pluim JP, Maintz JB, Viergever MA. Mutual-information-based registration of medical images: a survey. *IEEE Trans Med Imaging* 2003;22:986–1004.
16. Wimmer W, Venail F, Williamson T, et al. Semiautomatic cochleostomy target and insertion trajectory planning for minimally invasive cochlear implantation. *Biomed Res Int* 2014;2014:596498.
17. Holder JT, Kessler DM, Noble JH, et al. Prevalence of extracochlear electrodes: computerized tomography scans, cochlear implant maps, and operative reports. *Otol Neurotol* 2018;39:e325–31.

18. Timm ME, Majdani O, Weller T, et al. Patient specific selection of lateral wall cochlear implant electrodes based on anatomical indication ranges. *PLoS One* 2018;13:e0206435.
19. Pelliccia P, Venail F, Bonafé A, et al. Cochlea size variability and implications in clinical practice. *Acta Otorhinolaryngol Ital* 2014;34:42–9.
20. Landsberger D, Svrakic M, Roland T, Svirsky M. The relationship between insertion angles, default frequency allocations, and spiral ganglion place pitch in cochlear implants. *Ear Hear* 2015;36: e207–13.
21. Rivas A, Cakir A, Hunter J, et al. Automatic cochlear duct length estimation for selection of cochlear implant electrode arrays. *Otol Neurotol* 2017;38:339–46.
22. Wimmer W, Bell B, Huth M, et al. Cone beam and micro-computed tomography validation of manual array insertion for minimally invasive cochlear implantation. *Audiol Neurootol* 2014;19:22–30.